

# Atmospheric retrievals with the Tropospheric Emission Spectrometer (TES)

Kevin W. Bowman

August 11, 2003

## 1 Introduction

The Tropospheric Emission Spectrometer (TES) on the EOS-Aura spacecraft will measure the global 3-dimensional distribution of ozone in the troposphere and many of the chemical species that are part of its formation and destruction<sup>1</sup>. In particular, TES measurements will contribute to the understanding of the sources of ozone in the troposphere with implications for climate change, the oxidizing capacity of the atmosphere, and air quality on a global scale [WJ98, Cru95].

TES is a unique infrared Fourier Transform Spectrometer (FTS) in that it has both limb (side-looking) and nadir (down-looking) sounding capabilities [BGR01] as shown in Figure (1). TES will record the spectral radiance from the Earth's atmosphere at discrete locations, which are separated by about  $5^\circ$  along the orbit track, in the wavenumber range 650 to  $2250\text{ cm}^{-1}$ , ( $15.4$  to  $4.4\ \mu\text{m}$ ). Figure (2) shows the spectral radiance of the atmospheric species that TES can measure in the limb and nadir mode. The standard products that will be retrieved from these spectra are vertical concentration profiles of ozone, water vapor, carbon monoxide, methane, nitric oxide, and nitric acid.

## 2 Retrieval Approach

The estimation or "retrieval" of the vertical profiles of atmospheric constituents is based on an iterative minimization of the difference between a measured spectrum and a model spectrum evaluated at an atmospheric

---

<sup>1</sup>Information on the EOS-AURA platform can be found at <http://eos-chem.gsfc.nasa.gov/index.html>

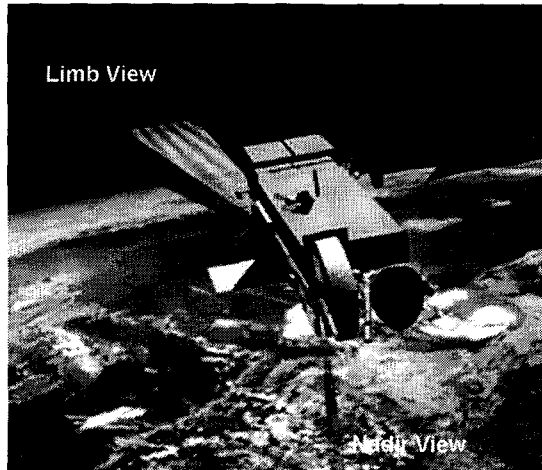


Figure 1: Nadir and limb modes on TES. In the nadir mode, the spatial resolution of TES is  $0.53 \times 5.3$  km with a swath of  $5.3 \times 8.5$  km. In the limb mode, TES has a height resolution of 2.3 km, with coverage from 0 to 34 km.

state subject to constraints that ensure a physically plausible solution. This iterative process is non-linear and can be computationally expensive. An analysis of errors for this algorithm is necessary to characterize the representation errors of the profile, choice of regularization, and the dependence of the retrieval error on both the statistics of the profile and spectral noise [BWS<sup>+</sup>02, Rod00].

Measured radiances in TES can be related to a forward model through the following additive noise model:

$$\mathbf{y} = \mathbf{F}(\mathbf{x}) + \mathbf{n} \quad (1)$$

where  $\mathbf{y} \in \mathbb{R}^N$ , is the calibrated, measured spectrum;  $\mathbf{x} \in \mathbb{R}^M$  is the "full" state vector whose elements are the atmospheric constituent defined on a log pressure grid. The forward model  $\mathbf{F} : \mathbb{R}^M \rightarrow \mathbb{R}^N$  simulates a spectrum produced from the propagation of radiation through the atmosphere from the Earth to the spacecraft. The noise term  $\mathbf{n} \in \mathbb{R}^N$  is assumed to be zero-mean, Gaussian white noise so that  $\mathbf{S}_n = E[\mathbf{nn}^T] = \sigma^2 \mathbf{I}$ , where  $E[\cdot]$  is the expectation operator [Pap84] and  $\sigma$  is the standard deviation of the noise.

The estimate of the atmospheric state is calculated from the solution of

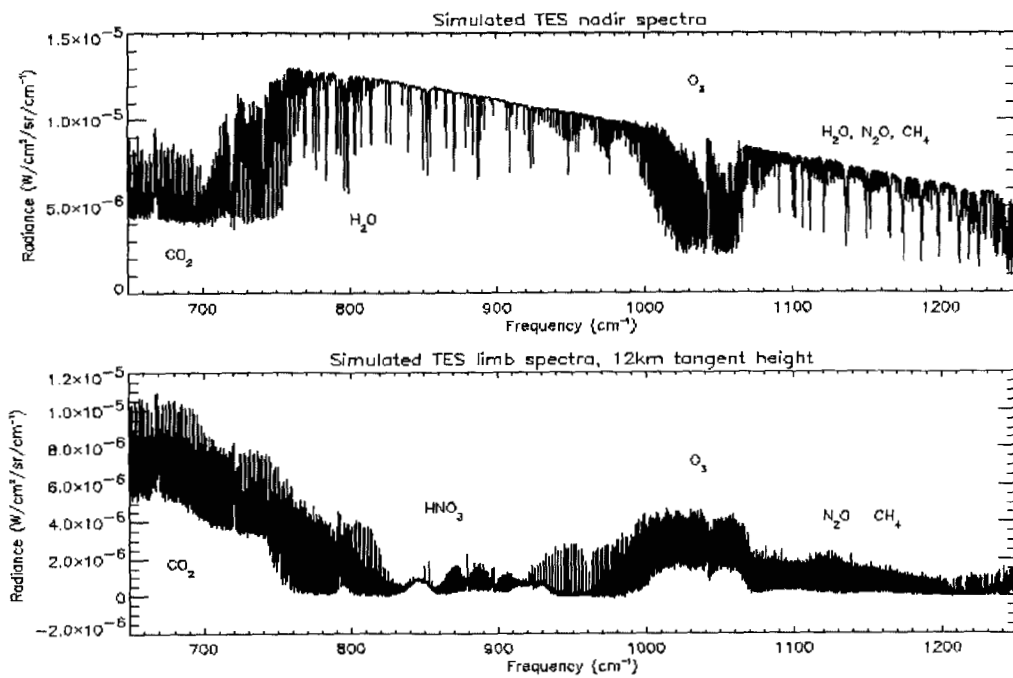


Figure 2: Spectral signatures of TES primary atmospheric species in nadir and limb modes.

the following regularized least squares problem:

$$\hat{\mathbf{x}} = \min_{\mathbf{x}} \left( \|\mathbf{y} - \mathbf{F}(\mathbf{x})\|_{\mathbf{S}_n^{-1}}^2 + \|\mathbf{x} - \mathbf{x}_c\|_{\Lambda}^2 \right) \quad (2)$$

where  $\mathbf{x}_c$  is the constraint vector and  $\Lambda \in \mathbb{R}^{M \times M}$  is the constraint matrix.

### 3 Application of retrievals to nadir and limb modes

In order to illustrate the retrieval approach, I have provided two simulated retrievals: one for nadir and one for limb. Figure (3) shows a simulated nadir retrieval of ozone from [BWS<sup>+</sup>02]. Ozone has a significant spectral radiance signature in  $\nu \in [985, 1075]\text{cm}^{-1}$  as indicated in Figure (2). The "true" ozone vertical distribution is substituted into Equation (1) along with Gaussian white noise, which has a standard deviation of  $\sigma = 1.32 \times 10^{-2} \text{W/m}^2/\text{sr/cm}^{-1}$ , in order to produce the "measured" radiances,  $\mathbf{y}$ . The initial guess vertical distribution of ozone,  $\mathbf{x}_0 = \mathbf{x}$ , and the constraint vector are substituted into Equation (2). The constraint matrix is based on a Twomey-Tikhonov-type smoothing constraint. The construction of this constraint and its strength relative to the data is described in [Ste02] and [SC01]. The retrieval is consistent with the true ozone above 20 km but is unable to capture the full extent of the variations in ozone between 5 and 20 km. Below 3 km, the estimated ozone distribution does not change from the constraint vector.

Limb retrievals are more challenging because the measured spectra are influenced by both the vertical and angular distribution of the atmospheric constituents. For this case, the atmospheric state vector,  $\mathbf{x}$ , is defined on a log pressure and angular grid. A 2-D distribution of carbon monoxide (CO) is shown in Figure (4). An estimate of this 2-D CO distribution is shown in Figure (5) and the constraint vector used is shown Figure (6). The constraint matrix chosen for this retrieval is based on the inverse of the climatological covariance of CO[WBJ03].

There are several questions we would like to address:

- Choice and strength of regularization,
- retrieval grid,
- error analysis.

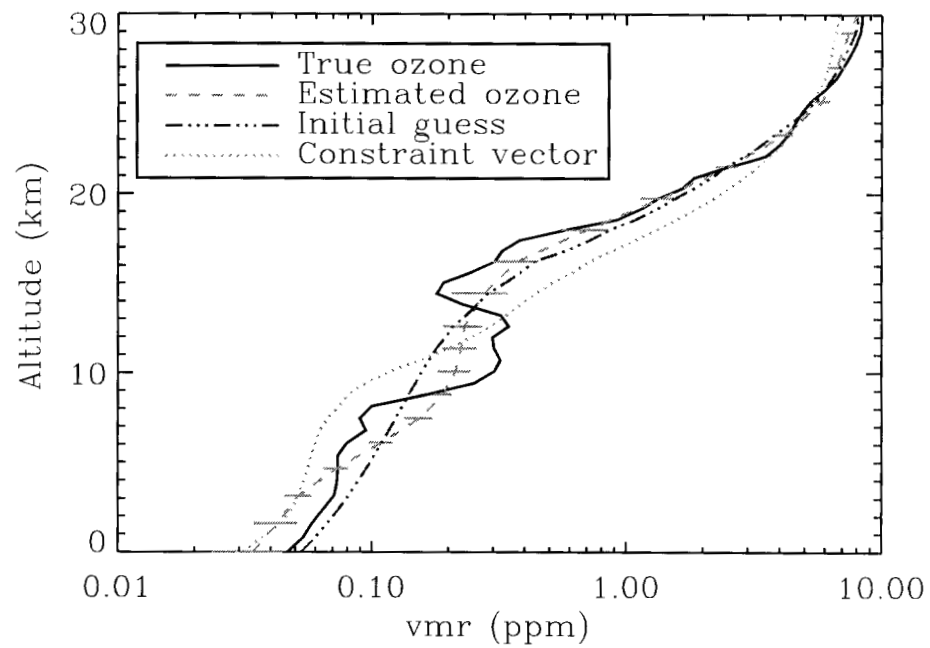


Figure 3: Retrieval of the April 30th ozonesonde profile. The figure shows the profile taken from the ozonesonde, the estimate of the ozone profile, the initial guess profile (the estimate from the shape retrieval), and the constraint profile (taken from climatology). The location of the retrieval levels are indicated by the error bars.

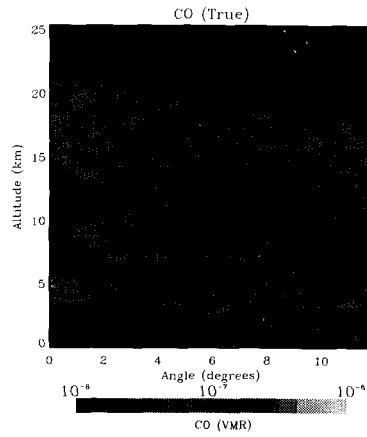


Figure 4: True CO distribution on an altitude and angular grid. The angular grid is based on Earth-centered coordinates. Each point in the image is the volume mixing ratio of CO at a specific altitude and angle with respect to the center of the Earth.

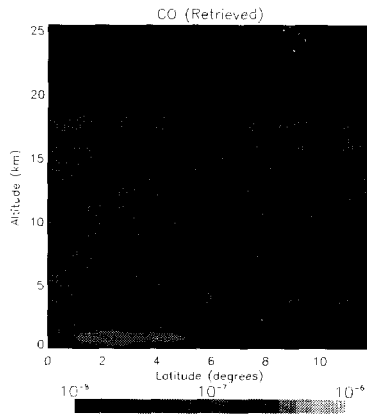


Figure 5: Retrieved inhomogeneous distribution of the CO atmospheric state.

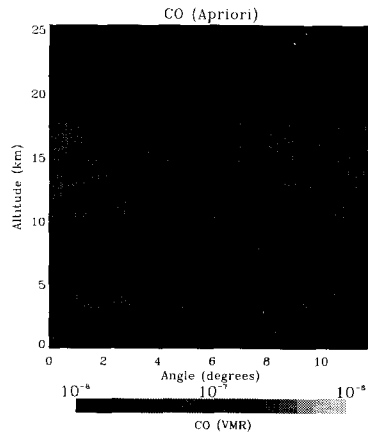


Figure 6: Constraint vector, which is chosen to be a homogenous distribution of CO.

## References

- [BGR01] R. Beer, T. Glavich, and D. Rider, *Tropospheric Emission Spectrometer for the Earth Observing System's Aura satellite*, *Applied Optics* **40** (2001), 2356–2367.
- [BWS<sup>+</sup>02] K. Bowman, J. Worden, T. Steck, H. Worden, S. Clough, and C. Rodgers, *Capturing time and vertical variability of tropospheric ozone: A study using tes nadir retrievals*, *J. Geophys. Res.* **107** (2002), no. D23, 4723.
- [Cru95] P. J. Crutzen, *Overview of tropospheric chemistry: Developments during the past quarter century and a look ahead*, *Faraday Discussions* (1995), no. 100, 1–21.
- [Pap84] A. Papoulis, *Probability, random variables, and stochastic processes*, McGraw-Hill, New York, 1984.
- [Rod00] C. Rodgers, *Inverse methods for atmospheric sounding: Theory and practise*, World Scientific, London, 2000.
- [SC01] T. Steck and T.v Clarmann, *Constrained profile retrieval applied to the observation mode of the Michelson Interferometer*

- for Passive Atmospheric Sounding*, Applied Optics **40** (2001), no. 21, 3559–3571.
- [Ste02] Tilman Steck, *Methods for determining regularization for atmospheric retrieval problems*, Applied Optics (2002), accepted for publication.
- [WBJ03] J. Worden, K. Bowman, and D. Jones, *Characterization of atmospheric profile retrievals from limb sounding observations of an inhomogeneous atmosphere*, JQSRT (2003), In press.
- [WJ98] Y. H. Wang and D. J. Jacob, *Anthropogenic forcing on tropospheric ozone and OH since preindustrial times*, Journal of Geophysical Research-Atmospheres **103** (1998), no. D23, 31123–31135.